Effective Permittivity of Shielding Composite Materials for Microwave Frequencies

Valentin Préault, Romain Corcolle, Laurent Daniel, and Lionel Pichon

***Abstract*—Due to mass constraints, composite materials are possible candidates to replace metal alloys for electromagnetic shielding applications. The design of standard metallic shielding enclosures often relies on finite-element calculations. But in the case of composite materials, the strong dependence on the shielding properties to the microstructure makes the finite-element approach almost impossible. Indeed meshing the microstructure would imply a huge number of elements, incompatible with usual computational resources. We propose in this paper to develop homogenization tools to define the effective electromagnetic properties of composite materials at microwave frequencies. The ratio between the characteristic size of the microstructure and the wavelength is shown to be a key parameter in the homogenization process. The effective properties can then be used as an input for electromagnetic compatibility standard tools, designed for homogeneous media.**

***Index Terms*—Effective medium, heterogeneous materials, homogenization, inclusion problem, Maxwell–Garnett model, shielding effectiveness.**

I. Introduction

THE number of electronic devices and wireless communication systems has significantly increased over the last 20 years. It is of major importance to manage electromagnetic compatibility (EMC) constraints at the design stage. Shielding enclosures are used to protect electronic devices from external radiations, but also to limit radiated emissions. Enclosures made of metal alloys—and particularly aluminum alloys—have often been used for that purpose and many numerical methods have been used to model the coupling between an electromagnetic (EM) wave and a 3-D enclosure with apertures. Examples of numerical methods are the finite-element method (FEM) [1], [2], the transmission-line modeling method [3], [4], the finite difference time domain (FDTD) method [5], [6], or the moment technique [7], [8]. The presence of metal is easily taken into account in these numerical methods by considering the material as a perfect electric conductor. Natural boundary conditions avoid the discretization of the thickness of the metallic sheets.

Manuscript received May 16, 2012; revised October 11, 2012; accepted May 16, 2013. Date of publication June 14, 2013; date of current version December 10, 2013. This work was supported by the project FUI-AAP10 SYRENA.

V. Préault, R. Corcolle, and L. Pichon are with the Laboratoire de Génie Électrique de Paris, CNRS (UMR 8507)/SUPELEC/UPMC/Univ Paris-Sud, 91192 Gif sur Yvette, France (e-mail: valentin.preault@lgep.supelec.fr; romain.corcolle@lgep.supelec.fr; lionel.pichon@lgep.supelec.fr).

L. Daniel is with the Laboratoire de Génie Électrique de Paris, CNRS (UMR 8507)/SUPELEC/UPMC/Univ Paris-Sud, 91192 Gif sur Yvette, France, and also with the School of Materials, University of Manchester, Manchester, M1 7HS, U.K. (e-mail: laurent.daniel@lgep.supelec.fr).

Color versions of one or more of the figures in this paper are available online at http://ieeexplore.ieee.org.

Digital Object Identifier 10.1109/TEMC.2013.2265173

The need to reduce the weight in aircraft and spacecraft industries promotes the use of composite materials such as carbon reinforced composites. When dealing with the modeling of such materials, two main difficulties arise.

The first difficulty concerns the conductivity of composite materials. Indeed, composite materials for EMC applications often contain conductive inclusions or fibers embedded in a dielectric medium. Such materials are not as electrically conductive as traditional metal structures and adequate models have to be developed in order to evaluate the shielding effectiveness (SE) of enclosures made from composite materials. For example, in [9]–[11], suitable models are proposed to take into account multilayered panels in the FDTD method. Other models are developed to simulate the behavior of simple heterogeneous sheets [12]–[16], modeled by homogeneous slabs characterized by effective permittivity and conductivity.

The second difficulty is the strong dependence on the shielding properties to the microstructure. Standard numerical methods allow accurate 3-D modeling of arbitrary shaped structures. But the need to refine the mesh of the enclosure down to the scale of the heterogeneities leads to prohibitive computational time and memory capacity for practical structures. In order to use numerical methods for EMC of composite shielding enclosures, effective properties have to be established for composite materials. These effective properties can then be introduced in numerical simulations instead of the heterogeneous microstructure. Many models for determining the effective EM properties of heterogeneous materials have been proposed [17], [18]. These models have mostly been established under static conditions. However, they are often used in dynamics and provide satisfying results as long as the wavelength remains large compared to the size of the heterogeneities [19]–[21]. Maxwell–Garnett (MG) estimate [22]–[26] is among the most popular models to compute the effective properties of composite materials in the case of EM excitation. It has been extended to higher frequencies [27] by including the skin-effect, the dimensional ratio in the resonance of fibers, and the Drude model. This model is useful at optical frequencies and limited to mixtures of randomly oriented conducting nanoparticles at concentrations far below the percolation threshold. Other models have been developed to enlarge the frequency range or to consider other distribution of phases, by using the multiple scattering theory [28] or the FEM over unit cells [29]–[31]. These methods require substantial computational time and resources to be performed.

Among alternative methods, experimental approaches have been proposed to measure the SE of composite enclosures [32]–[39]. But experimental techniques are not suitable during design processes due to cost and time constraints.

In this paper, we propose to extend quasi-static homogenization methods to define the equivalent homogeneous medium (EHM) for composite materials illuminated by an EM wave. This extension takes into account the influence of conductive phases diluted into a dielectric host matrix. It is shown that the frequency range of the proposed approach is extended by an order of magnitude compared to standard quasi-static homogenization methods in configurations studied in this paper.

In a first part, a reference configuration for the SE of a homogeneous sheet is reminded. The case of an heterogeneous material is then presented using the standard tools and the limitations of this approach are highlighted. The third part introduces the proposed adaptation of homogenization tools in order to account for the interaction between the incident wave and the microstructure of the composite material. The model validation is performed by comparison to simple configurations computed by FEM. A last part is dedicated to a discussion on the proposed approach in order to assess its range of validity.

II. SE of Homogeneous Materials

When a sheet is submitted to an EM perpendicular plane wave, part of the incident wave (E_I) is reflected (E_R), another is absorbed (E_A), and the third part is transmitted (E_T) through the material. The SE defines the attenuation between the incident and transmitted EM waves. It characterizes the behavior of a sheet subjected to an EM wave

$$\mathrm{SE} = 20 \log_{10} \frac{|E_I|}{|E_T|}. \tag{1}$$

A. Analytical Estimate

For some particular configurations, it is possible to compute SE for homogeneous media. The Appendix gives the analytical solution for the SE of an infinite homogeneous sheet illuminated by a perpendicular plane wave.

B. Finite-Element Estimate

SE for homogeneous media can also be calculated by FEM simulations. The commercial software COMSOL™ has been used to simulate the behavior of an homogeneous sheet submitted to an incident wave. To reduce the studied domain, we only consider a 2-D periodic cell. The simulation consists in illuminating the sheet by a perpendicular plain wave. Only a portion of the sheet is modeled, Neumann boundary condition [see Fig. 1(a)] is used to simulate an infinite sheet [40]. Two perfect matched layers (PML) are placed on both ends of the area modeled [see Fig. 1(b)]. These areas are used to simulate the presence of an infinite medium, especially without reflection, around the sheet [41].

C. Comparison Between Analytical and FEM Estimate

SE obtained by FEM and analytical calculations are compared in Fig. 2.

Analytical and FEM calculations are very close. The efficiency of the computations performed by FEM is limited when the SE is very high. In that case, the values of the transmitted wave are of the order of the numerical error. It appears around 180 dB. Hence, FEM results are not plotted above this threshold. It corresponds to $E_T/E_I \approx 10^{-9}$. In the following, when dealing with the EHM, the analytical calculation will be kept as the reference solution for the SE.

Fig. 1. Finite Element conditions. (a) Boundaries (bold line: incident wave, dotted: Neumann boundary condition, grey: continuity). (b) Subdomains (from left to right: PML / air / shielding sheet/ air / PML).

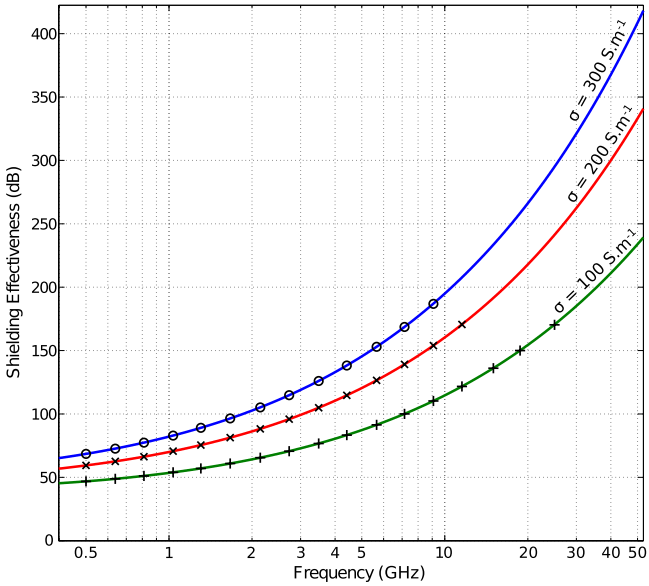

Fig. 2. Shielding effectiveness of homogeneous sheets with various conductivities σ: FEM (markers) and analytical (lines) results ($\mathrm{thickness} = 6$ mm, relative permittivity $\epsilon_r = 1$, relative permeability $\mu_r = 1$).

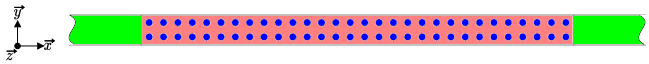

Fig. 3. 2D square microstructure studied.

III. SE of Heterogeneous Materials

In the case of heterogeneous materials, the SE depends on the properties of constituents, but also on the layout and on the shape of phases. The material considered in this paper (see Fig. 3) consists of a square array of long conductive parallel fibers (phase 2, electric conductivity σ_2, dielectric permittivity ϵ_2, magnetic permeability μ_2) surrounded by a dielectric matrix (phase 1, σ_1, ϵ_1, μ_1). Constituents are isotropic. Magnetic contrast is not considered here between the two phases ($\mu_1 = \mu_2$).

A. Finite-Element Approach

When considering such microstructures, FEM simulations require a precise refinement of the mesh involving high numbers of degrees of freedom and heavy computation time. Such requirements make this method uneasy to handle. Here, the infinite sheet will be modeled by a 2-D configuration. Calculations have been carried out on the microstructure shown in Fig. 3. Unlike the complete calculation of a shielding enclosure, it can be done with a reasonable computation time. The thickness of the plate is $l = 6$ mm and the fibers have a diameter ø$= 0.1$ mm. Fiber volume fraction is $f_2 = 19.63\%$. The calculation conditions are similar to those of Fig. 1 except that the shielding sheet is replaced by the heterogeneous microstructure.

SE of sheets made of carbon fibers in epoxy resins cannot be readily simulated by FEM with COMSOL™ because of the high conductivity of carbon ($\sigma_{\text{carbon}} \approx 65000$ S/m) inducing a huge number of elements to take into account the skin-depth effect in the inclusions and an SE above the 180 dB threshold. This is why lower conductivities have been considered in this paper.

B. Homogenization Methods

Homogenization consists in defining a fictive homogeneous medium (the EHM) equivalent to the composite material. The EHM exhibits on average the same behavior as the real heterogeneous medium. In the case of dielectric properties, assuming linear behavior, the constitutive law of each phase i can be written as

$$\mathbf{D}^i = \underline{\underline{\epsilon}}^i \cdot \mathbf{E}^i \tag{2}$$

where $\mathbf{D}^i$ and $\mathbf{E}^i$ are the electric induction and the electric field in the phase i. $\underline{\underline{\epsilon}}^i$ is the permittivity tensor of phase i.

The effective permittivity $\underline{\underline{\tilde{\epsilon}}}$ is defined by the relation between the average electric field $\overline{\mathbf{E}}$ and the average dielectric induction $\overline{\mathbf{D}}$ within the material [17]

$$\overline{\mathbf{D}} = \langle \mathbf{D}^i \rangle = \underline{\underline{\tilde{\epsilon}}} \cdot \overline{\mathbf{E}} = \underline{\underline{\tilde{\epsilon}}} \cdot \langle \mathbf{E}^i \rangle \tag{3}$$

where the operator $\langle . \rangle$ denotes an average operation over the volume.

The purpose of homogenization is to obtain the effective permittivity tensor $\underline{\underline{\tilde{\epsilon}}}$ from the knowledge of the properties and distribution of the constituents in the heterogeneous material. Homogenization methods are based on the study of a representative volume element (RVE). The size of the RVE must be as small as possible but large enough to be representative of the microstructure. It must be bigger than the heterogeneities, but small compared to the structure.

1) Inclusion-Based Methods: The method proposed in this paper relies on a static homogenization method built from basic inclusion problems [42], [43] (see Fig. 4). This method is briefly explained hereafter.

We consider an RVE of a multiphase material. Each phase of the material is supposed to behave on average as an homogeneous ellipsoidal inclusion embedded in an homogeneous infinite medium submitted to an external field $\mathbf{E}^0$. The properties of the infinite medium are noted $\underline{\underline{\epsilon}}^{\infty}$. It has been shown [43]

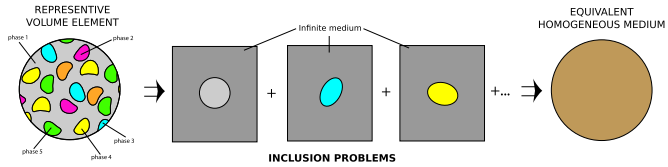

Fig. 4. Homogenization with inclusion problems.

that different choices of this permittivity tensor $\underline{\underline{\epsilon}}^{\infty}$ allow us to recover several classical estimates or bounds for the effective properties of the heterogeneous medium. The permittivity $\underline{\underline{\epsilon}}^i$ of the inclusion is the permittivity of the corresponding phase, and the shape of the inclusion is related to the spatial distribution of the phase in the heterogeneous material. The model is then based on the solution—analytical in some cases—of this elementary inclusion problem in the static case. In Mechanics, this problem is known as the Eshelby inclusion problem [44]. All these elementary problems are finally merged together to define the mean fields per phase in the heterogeneous medium.

In the inclusion problem, the relation between the internal $\mathbf{E}^i$ and applied $\mathbf{E}^0$ field is given by [43], [45], [46]

$$\mathbf{E}^i = \left(\underline{\underline{I}} + \underline{\underline{N}}^i \cdot \underline{\underline{\epsilon}}^{\infty -1} \cdot \left(\underline{\underline{\epsilon}}^i - \underline{\underline{\epsilon}}^{\infty} \right) \right)^{-1} \cdot \mathbf{E}^0 \tag{4}$$

where $\underline{\underline{N}}^i$ is the depolarization tensor for phase i [17] and $\underline{\underline{I}}$ is the second-order identity tensor. Using appropriate averaging operations [43], the effective permittivity tensor is expressed as

$$\underline{\underline{\tilde{\epsilon}}} = \left\langle \underline{\underline{\epsilon}}^i \cdot \left(\underline{\underline{I}} + \underline{\underline{N}}^i \cdot \underline{\underline{\epsilon}}^{\infty -1} \cdot \left(\underline{\underline{\epsilon}}^i - \underline{\underline{\epsilon}}^{\infty} \right) \right)^{-1} \right\rangle \cdot \left\langle \left(\underline{\underline{I}} + \underline{\underline{N}}^i \cdot \underline{\underline{\epsilon}}^{\infty -1} \cdot \left(\underline{\underline{\epsilon}}^i - \underline{\underline{\epsilon}}^{\infty} \right) \right)^{-1} \right\rangle^{-1}. \tag{5}$$

In the case of isotropic constituents, the effective permittivity $\tilde{\epsilon}_u$ in a direction $\mathbf{u}$ can be simplified:

$$\tilde{\epsilon}_u = \frac{\left\langle \dfrac{\epsilon^i}{\epsilon^{\infty} + N_u^i \left(\epsilon^i - \epsilon^{\infty} \right)} \right\rangle}{\left\langle \dfrac{1}{\epsilon^{\infty} + N_u^i \left(\epsilon^i - \epsilon^{\infty} \right)} \right\rangle} \tag{6}$$

where N_u^i is the projection of the tensor $\underline{\underline{N}}^i$ in direction $\mathbf{u}$ ($N_u^i = {}^t\mathbf{u} \cdot \underline{\underline{N}}^i \cdot \mathbf{u}$).

2) Biphasic Composites: The particular case of composite materials studied in this paper leads to further simplifications. For a biphasic composite with isotropic constituents of volume fraction f_i ($f_1 + f_2 = 1$), $\underline{\underline{N}}^1 = \underline{\underline{N}}^2 = \underline{\underline{N}}$ and the effective permittivity in direction $\mathbf{u}$ is given by

$$\tilde{\epsilon}_u = \frac{\epsilon_1 \dfrac{f_1}{\epsilon^{\infty} + N_u \left(\epsilon_1 - \epsilon^{\infty} \right)} + \epsilon_2 \dfrac{f_2}{\epsilon^{\infty} + N_u \left(\epsilon_2 - \epsilon^{\infty} \right)}}{\dfrac{f_1}{\epsilon^{\infty} + N_u \left(\epsilon_1 - \epsilon^{\infty} \right)} + \dfrac{f_2}{\epsilon^{\infty} + N_u \left(\epsilon_2 - \epsilon^{\infty} \right)}}. \tag{7}$$

The choice of the properties of the matrix for the permittivity of the infinite medium ($\epsilon^{\infty} = \epsilon_1$), suggested in the mechanical model of Mori–Tanaka [49], provides a good estimate of the effective properties for this type of microstructure with low concentration of fibers. This choice gives the following estimate

for the effective permeability:

$$\tilde{\epsilon}_u = \epsilon_1 + f_2\epsilon_1 \frac{\epsilon_2 - \epsilon_1}{\epsilon_1 + f_1 N_u(\epsilon_2 - \epsilon_1)}. \tag{8}$$

If in addition the material is made of a matrix surrounding long parallel fibers aligned along direction **z**, the distribution of constituents is transversely isotropic. The corresponding shape for the inclusion in the elementary problem is an infinite cylinder. The corresponding depolarization tensor is [17]

$$\underline{\underline{N}} = \begin{bmatrix} 1/2 & 0 & 0 \\ 0 & 1/2 & 0 \\ 0 & 0 & 0 \end{bmatrix}. \tag{9}$$

The effective permittivity in the directions perpendicular to the fibers can be written from (7):

$$\tilde{\epsilon}_\perp = \frac{\epsilon_1 \dfrac{f_1}{\epsilon^\infty + \epsilon_1} + \epsilon_2 \dfrac{f_2}{\epsilon^\infty + \epsilon_2}}{\dfrac{f_1}{\epsilon^\infty + \epsilon_1} + \dfrac{f_2}{\epsilon^\infty + \epsilon_2}}. \tag{10}$$

Applying the choice of Mori–Tanaka model for the infinite medium in this equation ($\epsilon^\infty = \epsilon_1$) reduces to the standard MG model (11) for the permittivity in the directions perpendicular to the fibers, and to the Wiener estimate (12) for the permittivity in the direction parallel to the fibers:

$$\tilde{\epsilon}_\perp = \epsilon_1 + 2f_2\epsilon_1 \frac{\epsilon_2 - \epsilon_1}{\epsilon_1 + \epsilon_2 - f_2(\epsilon_2 - \epsilon_1)} \tag{11}$$

$$\tilde{\epsilon}_{//} = f_1\epsilon_1 + f_2\epsilon_2. \tag{12}$$

C. Case of Harmonic Excitation

When considering harmonic solicitations, the equations above can be used by replacing the permittivity tensor by its complex expression $\underline{\underline{\epsilon}}^*$ depending on the material permittivity $\underline{\underline{\epsilon}}$ and conductivity $\underline{\underline{\sigma}}$ and on the angular frequency ω of the incident wave

$$\underline{\underline{\epsilon}}^* = \underline{\underline{\epsilon}} + \frac{1}{j\omega}\underline{\underline{\sigma}}. \tag{13}$$

In the following, the complex permittivity will always be used for the homogenization modeling.

D. Comparison Between Finite Element and Homogenization Techniques

The FEM calculation has been performed on the microstructure presented in Fig. 3. The homogenization has been performed according to the inclusion-based model and the corresponding EHM properties have been introduced in the analytical expression of the SE for an infinite sheet. The agreement between the analytical model and FEM in the case of an homogeneous sheet has been previously verified (see Fig. 2) so that this comparison is clearly related to the accuracy of the homogenization model. The results are presented in Figs. 5 and 6. When the electric field is oriented in the fibers direction (**z**), Wiener model provides an accurate estimate when compared to FEM result (see Fig. 5). This result is related to the homogeneity

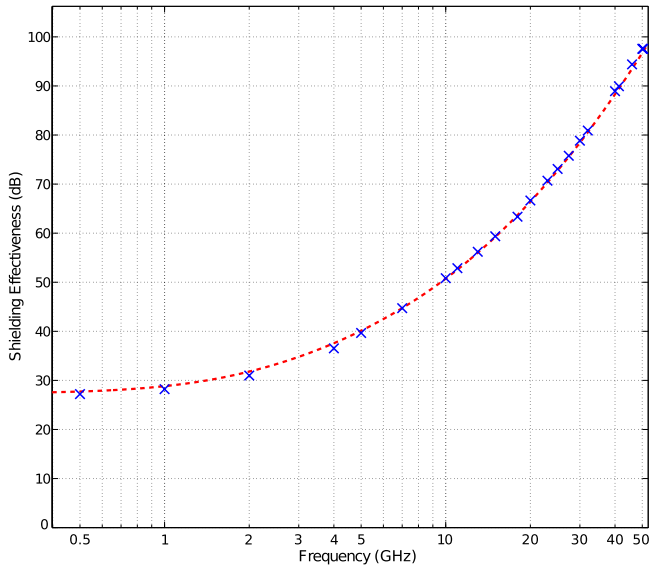

Fig. 5. Shielding effectiveness of an infinite sheet (microstructure of Fig. 3) as a function of the frequency of the incident wave: FEM (crosses) and Wiener (dashed line) results. Configuration: electric field oriented parallel to the fibers, $\emptyset = 0.1$ mm, $\sigma_1 = 1$ S.m^{-1}, $\sigma_2 = 100$ S.m^{-1}, $\epsilon_1 = 5\epsilon_0$, $\epsilon_2 = \epsilon_0$, $\mu_1 = \mu_2 = \mu_0$.

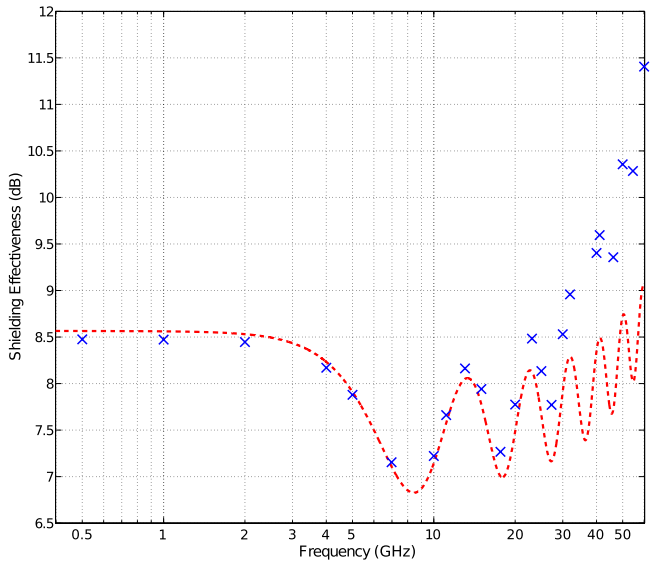

Fig. 6. Shielding effectiveness of an infinite sheet (microstructure of Fig. 3) as a function of the frequency of the incident wave: FEM (crosses) and MG (dashed line) results. Configuration: electric field oriented perpendicularly to the fibers, $\emptyset = 0.1$ mm, $\sigma_1 = 1$ S.m^{-1}, $\sigma_2 = 1000$ S.m^{-1}, $\epsilon_1 = 5\epsilon_0$, $\epsilon_2 = \epsilon_0$, $\mu_1 = \mu_2 = \mu_0$.

of the root mean square of the electric field in each phase for this particular configuration when no skin effect is involved.

When the electric field is perpendicular to the fibers, MG model leads to very significant discrepancies compared to FEM simulations (see Fig. 6). At high frequencies (above 10 GHz), the SE provided by the homogeneous sheet made of effective properties is not the same as the SE provided by the heterogeneous sheet computed by FEM. The standard MG model does not take into account the interactions between the microstructure and the EM wave. An extension of quasi-static homogenization

tools is needed to describe the effective properties for composite materials at high frequencies.

IV. Homogenization Estimate for Dynamic Excitation

A. Adaptation to Dynamic Conditions

When the frequency increases, the characteristic size of the phases has an influence on the behavior of the material. Thus, it is necessary to introduce in the modeling a length parameter, inexistent in standard mean field approaches. The proposed approach to adapt the inclusion based homogenization method is empirical: several finite-element computations were performed at different frequencies and for different diameters of fibers. From each of these computations, an optimal infinite medium has been identified for the homogenization model. The properties of the infinite medium were found to be mainly sensitive to the conductivity. Because the fibers are much more conductive than the matrix in the cases studied, the complex permittivity of the fibers has been added to Mori–Tanaka infinite medium

$$\epsilon^{\infty} = \epsilon_1^* + \epsilon_2^* \times A. \tag{14}$$

The ratio γ/λ has been introduced to compare the typical size γ of the microstructure and the typical length λ of the wave. When the optimal conductivity of the infinite medium is plotted as a function of the frequency, it is shown that a square dependence on the frequency is a reasonable approximation. Thus, the infinite medium permittivity is chosen as

$$\epsilon^{\infty} = \epsilon_1^* + \epsilon_2^* \times \left(\frac{\gamma}{\lambda}\right)^2 \tag{15}$$

where λ is the wavelength in the effective medium and γ is the characteristic size of the microstructure. In our case, γ is the fiber diameter. At low frequency, the corresponding dynamic homogenization model (DHM) provides estimates similar to standard static homogenization tools because λ is very large compared to γ. Therefore, the second part of (15) vanishes. In the general case, due to the choice of ϵ^{∞}, λ depends on the effective properties. The model should then be iterative. However, the wavelength corresponding to the MG static estimate was used. The convergence is then reached very fast and the accuracy of the model is not affected by neglecting the iterative process. The relative error remains lower than 0.02% in the calculations performed below. It is recalled that we do not consider here any magnetic contrast between the phases of the composite material: $\mu_1 = \mu_2$.

Introducing our choice of infinite medium (15) in (10) leads to a new estimate for the EHM in the perpendicular directions:

$$\tilde{\epsilon}_{\perp} = \frac{\epsilon_1^* \dfrac{f_1}{2\epsilon_1^* + \epsilon_2^* \times \left(\dfrac{\gamma}{\lambda}\right)^2} + \epsilon_2^* \dfrac{f_2}{\epsilon_1^* + \epsilon_2^* \times \left(\left(\dfrac{\gamma}{\lambda}\right)^2 + 1\right)}}{\dfrac{f_1}{2\epsilon_1^* + \epsilon_2^* \times \left(\dfrac{\gamma}{\lambda}\right)^2} + \dfrac{f_2}{\epsilon_1^* + \epsilon_2^* \times \left(\left(\dfrac{\gamma}{\lambda}\right)^2 + 1\right)}}. \tag{16}$$

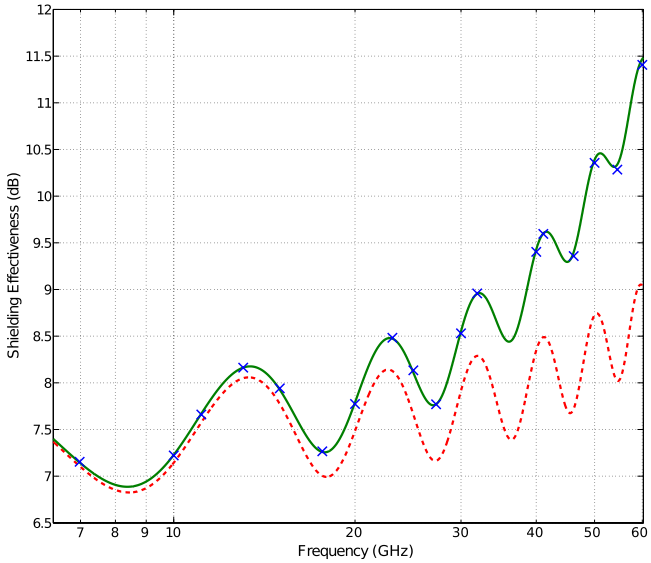

Fig. 7. Shielding effectiveness of an infinite sheet (microstructure of Fig. 3) as a function of the frequency of the incident wave: FEM (crosses), MG (dashed line) and DHM (line) results. Configuration: idem as Fig. 6.

B. Results

Using the DHM presented above, and following the same approach as above, the SE of the composite material can be estimated and compared to the FEM estimate. For a given frequency, the computation time to define the SE of an heterogeneous sheet by FEM is about 45 s on a standard workstation. It is reduced to 0.9 s for an homogeneous sheet. The use of the full analytical method (Homogenization and analytical formula for SE) is almost instantaneous (a few milliseconds). The computation time is then estimated between 3000 and 4000 times faster when using the full analytical approach compared to the heterogeneous FEM computation.

When the electric field is oriented along the fibers direction (**z**), the choice of the infinite medium has no influence on the properties of the EHM because the corresponding term of the depolarization tensor is zero. The dynamic model is then equivalent to Wiener models and provides the result shown in Fig. 5. When the electric field is perpendicular to the fibers (direction **y**), the dynamic term in the infinite medium permittivity (15) provides a correction of the effective medium properties at high frequency (see Fig. 7). The dynamic correction term significantly enhances the prediction of the SE of the composite material.

If we consider the reflected wave plotted in Fig. 8 ($RW = 20\log_{10}\frac{|E_I|}{|E_R|}$; see the Appendix), the DHM also provides a more accurate prediction than the standard MG static model. Again, the addition in the elementary inclusion problem of a correction term depending on the characteristic size of the microstructure and on the frequency leads to significant improvement.

V. Discussion

Using the DHM, the EMC efficiency of various heterogeneous materials can be evaluated. The analysis in this part is

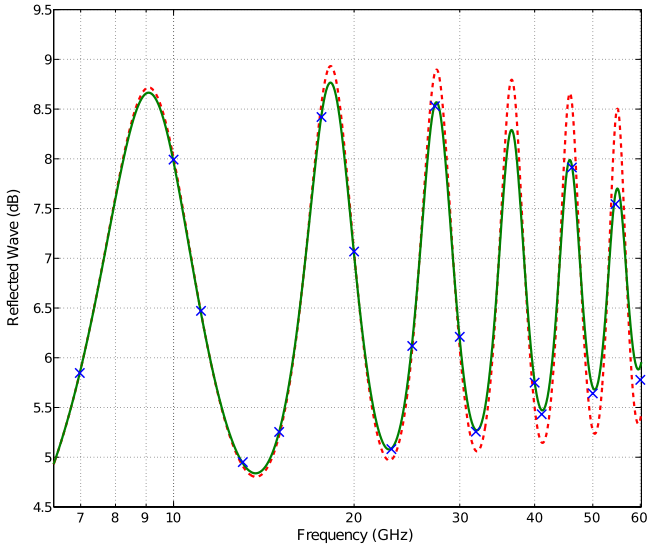

Fig. 8. Reflected wave on an infinite sheet (microstructure of Fig. 3) as a function of the frequency of the incident wave: FEM (crosses), MG (dashed line) and DHM (line) results. Configuration: idem as Fig. 6.

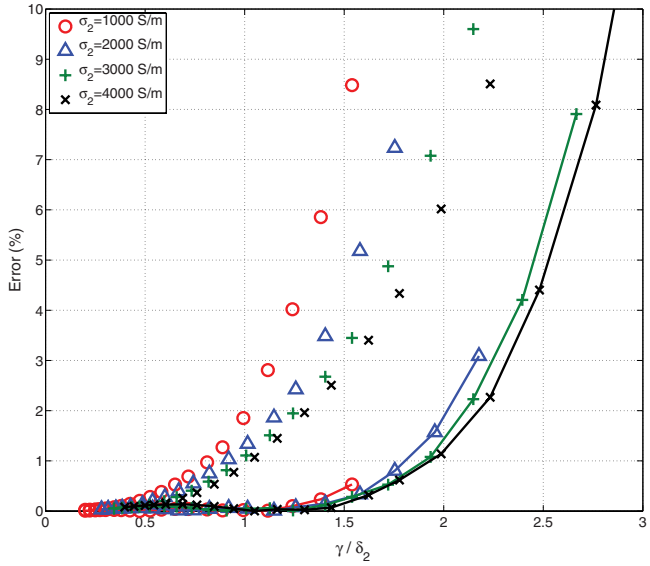

Fig. 9. Relative error between the SE computed by FEM and MG (markers only) and the DHM (lines with markers). The electric field is oriented perpendicular to the fibers ($\text{ø} = 0.1$ mm, $\sigma_1 = 1\text{S.m}^{-1}$, $\epsilon_1 = 5\epsilon_0$, $\epsilon_2 = \epsilon_0$, $\mu_1 = \mu_2 = \mu_0$). Microstructure of Fig. 3. Calculations between $500Mhz$ and $60GHz$.

restricted to biphasic composite sheets with isotropic constituents in isotropic distribution. The purpose is to identify the first limitations of this approach.

A. Particle Size or Frequency Effect

Keeping the calculations within the range of validity of the FEM, the relative difference between the SE computed by FEM and the DHM is plotted in Fig. 9 as a function of the ratio between the characteristic size of the microstructure γ and the skin depth δ_2 of the conductive material.

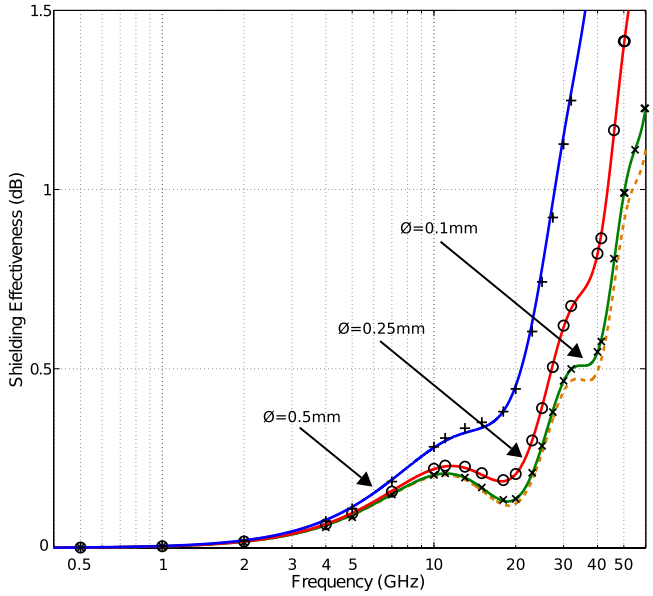

Fig. 10. Shielding effectiveness of sheets (square microstructures) with various fiber diameters ø: FEM (markers), MG (dashed line) and DHM (lines) results. Configuration: electric field oriented perpendicularly to the fibers, $f_2 = 19.63\%$, $\sigma_1 = 1e-20$ S.m^{-1}, $\sigma_2 = 100$ S.m^{-1}, $\epsilon_1 = \epsilon_2 = \epsilon_0$, $\mu_1 = \mu_2 = \mu_0$.

$$\delta_2 = \sqrt{\frac{2}{\mu_2 \sigma_2 \omega}} \tag{17}$$

Many articles (see, e.g., [47] and [48]) mention that homogenization techniques get inaccurate when the frequency of the incident field gets too high or when the heterogeneities become too big. However, this information is rarely quantitatively assessed. Fig. 9 shows that, under the conditions considered in this paper, the error on the SE for the MG estimate becomes significant (more than 0.5%) as soon as the skin depth reaches two times the characteristic size of the inclusions. Indeed under such conditions, eddy currents are located on the surface of the fibers. Inner and outer parts of the volume of the fibers are electrically loaded in a very different way. The validity criterion of MG estimate could be defined as $\gamma < 1/2\ \delta_2$. When using the DHM, the validity range is pushed up to $\gamma < 3/2\ \delta_2$ for the same criterion. Above this value, the appropriate length to be introduced in the model is not the typical size of the fibers, but should rather be related to the skin depth. In other words, using (17), it can be said that the proposed expression (15) for the infinite medium properties allows us to increase the frequency range by almost one order of magnitude compared to standard quasi-static homogenization models for the cases computed in this study.

Fig. 10 compares the efficiency of three sheets with the same volume fraction of fibers but with different diameters. The MG model gives the same results for the three microstructures since it does not take into consideration the diameter of the inclusions. FEM calculations show that the SE increases with fiber diameter and the DHM captures this effect. If the size of the fibers gets

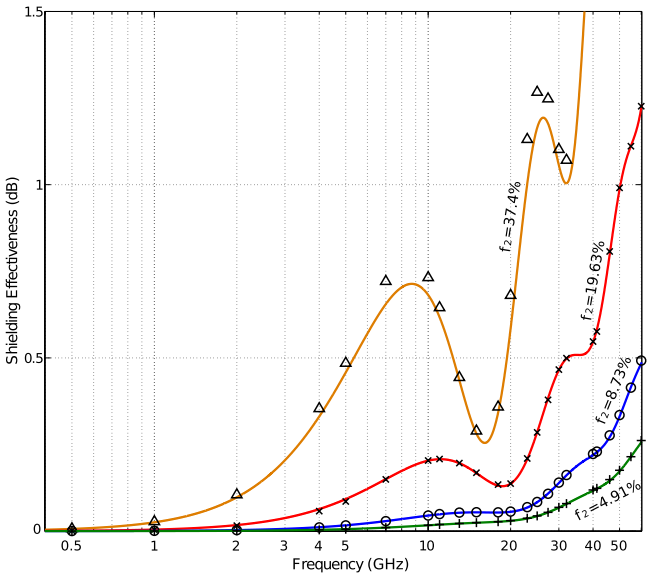

Fig. 11. Shielding effectiveness of sheets (square microstructures) with various amount of fiber f_2: FEM (markers) and DHM (lines) results. Configuration: electric field oriented perpendicular to the fibers, $\varnothing = 0.1$ mm, $\sigma_1 = 1e-20$ S.m^{-1}, $\sigma_2 = 100$ S.m^{-1}, $\epsilon_1 = \epsilon_2 = \epsilon_0$, $\mu_1 = \mu_2 = \mu_0$.

too large, similar effects to those observed when increasing the frequency would be noticed.

B. Particle Concentration Effect

Fig. 11 shows the SE of composite sheets with identical fiber size but different concentrations. The electrical field is oriented perpendicular to the fibers. As expected, the higher the amount of conductive fibers, the higher the SE.

For high fiber volume fraction ($f_2 > 20\%$), the DHM becomes inaccurate. The reason is related to the choice of the infinite medium. The choice of the matrix permittivity for $\underline{\underline{\epsilon}}^{\infty}$, inspired by the Mori–Tanaka model in Mechanics [49] is known to be relevant only for dilute systems [42]. When the volume fraction is getting higher, this choice is not appropriate and a self-consistent (or Bruggeman) approach should be preferred. This point is part of a work in progress.

VI. Conclusion

This paper is dedicated to the determination of the effective properties of composite materials for EMC applications. The limitations of standard static homogenization tools in this context are highlighted. A DHM is proposed to overcome these limitations. This model can be seen as an extension of MG model to higher frequencies by the introduction of a length parameter. This length parameter is relative to the typical size of the microstructure of the composite material. The model has been tested on an example of fiber-matrix composite. It is shown to provide accurate results as long as the volume fraction of the fibers remains low and the radius of the fibers remains below the skin depth of the fibers. This modeling approach can be extended to a large range of microstructures. Further studies will be undertaken on how shape and distribution of phases influence the SE. The benefit of this approach is the small computation time required to obtain the effective properties of composite materials. These properties can then be readily implemented in FEM tools to simulate the complete SE of complex enclosures.

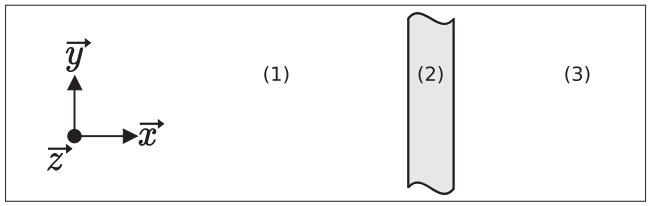

Fig. 12. Scheme of studied domain ((1) and (3): air, (2): infinite sheet).

Appendix
EMC Properties of an Infinite Homogeneous Sheet

The particular case of an infinite sheet (see Fig. 12) allows analytical calculations of the SE and reflected wave [45]. We consider an homogeneous isotropic sheet of constant thickness l submitted to a progressive monochromatic polarized plane wave with angular frequency ω and normal incidence. No assumption is considered on the properties of the sheet (not perfectly conducting neither perfectly dielectric).

A. Shielding Effectiveness

The SE of the infinite sheet can be divided into three parts:

$$\mathrm{SE} = \mathrm{SE}_A + \mathrm{SE}_B - \mathrm{SE}_R. \tag{18}$$

The wave attenuation is first caused by the absorption of the material:

$$\mathrm{SE}_A = 20\log_{10}\left|e^{(k+k_0)l}\right| \tag{19}$$

with $k = \sqrt{\epsilon\mu\omega^2 - j\mu\sigma\omega}$ the wave vector, $k_0 = \frac{\omega}{c}$ the wave vector in air ($c = 3.10^8$ m $\cdot$ s^{-1}), ϵ the dielectric permittivity, σ the electric conductivity, and μ the magnetic permeability. The second part is reflected by the sheet:

$$\mathrm{SE}_R = 20\log_{10}|p| \tag{20}$$

with $p = \frac{4\frac{n}{\mu_r}}{(\frac{n}{\mu_r}+1)^2}$ the transmission coefficient, $n = \frac{k}{k_0}$ the refractive index of the medium, and μ_r the relative permeability ($\mu = \mu_r\mu_0$). The third part corresponds to multiple reflections inside the material. It is negative:

$$\mathrm{SE}_B = 20\log_{10}\left|1 - q^2 \times e^{-2kl}\right| \tag{21}$$

with $q = \frac{\frac{n}{\mu_r}-1}{\frac{n}{\mu_r}+1}$ the reflection coefficient.

B. Reflected Wave

The reflected wave can also be defined

$$E_R = E_I \times \frac{q}{1 - q^2 \times e^{-2kl}} \times \left(1 - e^{-2kl}\right). \tag{22}$$

As for the SE, it can be expressed as a ratio

$$RW = 20\log_{10}\frac{|E_I|}{|E_R|}. \tag{23}$$

When developed, this expression gives

$$RW = 20\log_{10}\left|\frac{1-q^2\times e^{-2kl}}{q}\right| - 20\log_{10}\left|1-e^{-2kl}\right|. \tag{24}$$

REFERENCES

[1] S. Celozzi and M. S. Sarto, "Equivalent source method for the evaluation of the electromagnetic field penetration inside enclosures," *IEEE Trans. Magn.*, vol. 32, no. 3, pp. 1497–1500, May 1996.

[2] W. P. Carpes, L. Pichon, and A. Razek, "Analysis of the coupling of an incident wave with a wire inside a cavity using an FEM in frequency and time domains," *IEEE Trans. Electromagn. Compat.*, vol. 44, no. 3, pp. 470–475, Aug. 2002.

[3] W. P. Carpes, G. S. Ferreira, A. Raizer, L. Pichon, and A. Razek, "TLM and FEM methods applied in the analysis of electromagnetic coupling," *IEEE Trans. Magn.*, vol. 36, no. 4, pp. 982–985, Jul. 2000.

[4] B. L. Nie, P. A. Du, Y. T. Yu, and Z. Shi, "Study of the shielding properties of enclosures with apertures at higher frequencies using the transmission-line modeling method," *IEEE Trans. Electromagn. Compat.*, vol. 53, no. 1, pp. 73–81, Feb. 2011.

[5] M. Kuang-Pin, L. Min, J. L. Drewniak, T. H. Hubing, and T. P. van Doren, "Comparison of FDTD algorithms for subcellular modeling of slots in shielding enclosures," *IEEE Trans. Electromagn. Compat.*, vol. 39, no. 2, pp. 147–155, May 1997.

[6] L. Min, J. Nuebel, J. L. Drewniak, R. E. Dubroff, T. H. Hubing, and T. P. van Doren, "EMI from cavity modes of shielding enclosures-FDTD modeling and measurements," *IEEE Trans. Electromagn. Compat.*, vol. 42, no. 1, pp. 29–38, Feb. 2000.

[7] Z. B. Zhao, X. Cui, L. Li, and B. Zang, "Analysis of the shielding effectiveness of rectangular enclosure of metal structures with apertures above ground plane," *IEEE Trans. Magn.*, vol. 41, no. 5, pp. 1892–1895, May 2005.

[8] M. A. Khorrami, P. Dehkhoda, R. M. Mazandaran, and S. Sadeghi, "Fast shielding effectiveness calculation of metallic enclosures with apertures using a multiresolution method of moments technique," *IEEE Trans. Electromagn. Compat.*, vol. 52, no. 1, pp. 230–235, Feb. 2010.

[9] M. S. Sarto, "A new model for the FDTD analysis of the shielding performances of thin composite structures," *IEEE Trans. Electromagn. Compat.*, vol. 41, no. 4, pp. 298–306, Nov. 1999.

[10] M. D'Amore and M. S. Sarto, "Theoretical and experimental characterization of the EMP-interaction with composite-metallic enclosures," *IEEE Trans. Electromagn. Compat.* vol. 42, no. 2, pp. 152–163, May 2000.

[11] C. Jiao, L. Li, X. Cui, and H. Li, "Subcell FDTD analysis of shielding effectiveness of a thin-walled enclosure with an aperture," *IEEE Trans. Electromagn. Compat.*, vol. 42, no. 4, pp. 1075–1078, Apr. 2006.

[12] M.-S. Lin and C. H. Chen, "Plane-wave shielding characteristics of anisotropic laminated composites," *IEEE Trans. Electromagn. Compat.*, vol. 35, no. 1, pp. 21–27, Feb. 1993.

[13] M.-S. Lin, C. M. lin, R. B. Wu, and C. H. Chen, 'Transient propagation in anisotropic laminated composites," *IEEE Trans. Electromagn. Compat.*, vol. 35, no. 3, pp. 357–365, Aug. 1993.

[14] H. C. Chu and C. H. Chen, "Shielding and reflection properties of periodic fiber-matrix composite structures," *IEEE Trans. Electromagn. Compat.*, vol. 38, no. 1, pp. 1–6, Feb. 1996.

[15] H. K. Chiu, M. S. Lin, and C. H. Chen, "Near-field shielding and reflection characteristics of anisotropic laminated planar composites," *IEEE Trans. Electromagn. Compat.*, vol. 39, no. 4, pp. 332–339, Nov. 1997.

[16] H. K. Chin, H. C. Chu, and C. H. Chen, "Propagation modeling of periodic laminated composite structures," *IEEE Trans. Electromagn. Compat.*, vol. 40, no. 3, pp. 218–224, Aug. 1998.

[17] A. Sihvola, *Electromagnetic Mixing Formulas and Application* (IEE Electromagnetic Waves Series 47). London, U.K.: IET, 1999.

[18] G. W. Milton, *The Theory of Composites*. Cambridge, U.K.: Cambridge Univ. Press, 2002.

[19] C. L. Holloway, M. S. Sarto, and M. Johansson, "Analyzing carbon-fiber composite materials with equivalent-layer models," *IEEE Trans. Electromagn. Compat.*, vol. 47, no. 4, pp. 833–844, Nov. 2005.

[20] E. F. Kuester and C. L. Holloway, "Comparison of approximations for effective parameters of artificial dielectrics," *IEEE Trans. Microw. Theory Tech.*, vol. 38, no. 11, pp. 1752–1755, Nov. 1990.

[21] E. F. Kuester and C. L. Holloway, "A low-frequency model for wedge or pyramid absorber arrays—I: Theory," *IEEE Trans. Electromagn. Compat.*, vol. 36, no. 4, pp. 300–306, Nov. 1994.

[22] I. M. De Rosa, R. Mancinelli, F. Sarasini, M. S. Sarto, and A. Tamburrano, "Electromagnetic design and realization of innovative fiber-reinforced broad-band absorbing screens," *IEEE Trans. Electromagn. Compat.*, vol. 51, no. 3, pp. 700–707, Aug. 2009.

[23] M. Y. Koledintseva, J. Drewniak, R. Dubroff, K. Rozanov, and B. Archambeault, "Modelling of shielding composite materials and structures for microwave frequencies," *Progr. Electromagn. Res. B*, vol. 15, pp. 197–215, 2009.

[24] P. P. Kuzhir, A. G. Paddubskaya, S. A. Maksimenko, V. L. Kuznetsov, S. Moseenkov, A. I. Romanenko, O. A. Shenderova, J. Macutkevic, G. Valusis, and P. Lambin, "Carbon onion composites for EMC applications," *IEEE Trans. Electromagn. Compat.*, vol. 54, no. 1, pp. 6–16, Feb. 2012.

[25] M. S. Sarto, A. G. D'Aloia, A. Tamburrano, and G. De Bellis, "Synthesis, modeling, and experimental characterization of graphite nanoplatelet-based composites for EMC applications," *IEEE Trans. Electromagn. Compat.*, vol. 54, no. 1, pp. 17–27, Feb. 2012.

[26] M. H. Nisanci, F. de Paulis, M. Y. Koledintseva, J. L. Drewniak, and A. Orlandi, "From Maxwell Garnett to Debye Model for electromagnetic simulation of composite dielectrics-part II: Random cylindrical inclusions," *IEEE Trans. Electromagn. Compat.*, vol. 54, no. 2, pp. 280–289, Apr. 2012.

[27] M. Y. Koledintseva, R. E. DuBroff, and R. W. Schwartz, "A Maxwell Garnett model for dielectric mixtures containing conducting particles at optical frequencies," *Progr. Electromagn. Res.*, vol. 63, pp. 223–242, 2006.

[28] L. Tsang and J. A. Kong, "Multiple scattering of electromagnetic waves by random distributions of discrete scatterers with coherent potential and quantum mechanical formalism," *J. Appl. Phys.*, vol. 51, pp. 3465–3485, 1980.

[29] B. Sareni, L. Krahenbuhl, A. Beroual, and C. Brosseau, "Complex effective permittivity of a lossy composite material," *J. Appl. Phys.*, vol. 80, pp. 4560–4565, 1996.

[30] B. Sareni, L. Krahenbuhl, A. Beroual, and C. Brosseau, "Effective dielectric constant of random composite materials," *J. Appl. Phys.*, vol. 81, pp. 2373–2383, 1997.

[31] M. El Feddi, Z. Ren, A. Razek, and A. Bossavit, "Homogenization technique for Maxwell equations in periodic structures," *IEEE Trans. Magn.*, vol. 33, no. 2, pp. 1382–1385, Mar. 1997.

[32] C. L. Gardner and Y. F. C. Poissant, "Measurement of the shielding properties of composite materials: Comparison of the dual TEM and noncontact probe methods," *IEEE Trans. Electromagn. Compat.*, vol. 40, no. 4, pp. 364–369, Nov. 1998.

[33] P. B. Jana, A. K. Mallik, and S. K. De, "Effects of sample thickness and fiber aspect ratio on EMI shielding effectiveness of carbon fiber filled polychloroprene composites in the X-band frequency range," *IEEE Trans. Electromagn. Compat.*, vol. 34, no. 4, pp. 478–481, Nov. 1992.

[34] U. Lundgren, J. Ekman, and J. Delsing, "Shielding effectiveness data on commercial thermoplastic materials," *IEEE Trans. Electromagn. Compat.*, vol. 48, no. 4, pp. 766–773, Nov. 2006.

[35] A. L. Bogorad, M. P. Deeter, K. A. August, G. Doorley, J. J. Likar, and R. Herschitz, "Shielding effectiveness and closeout methods for composite spacecraft structural panels," *IEEE Trans. Electromagn. Compat.*, vol. 50, no. 3, pp. 547–555, Aug. 2008.

[36] I. M. De Rosa, F. Sarasini, M. S. Sarto, and A. Tamburrano, "EMC impact of advanced carbon fiber/carbon nanotube reinforced composites for next-generation aerospace applications," *IEEE Trans. Electromagn. Compat.*, vol. 50, no. 3, pp. 556–563, Aug. 2008.

[37] D. A. Lampasi and M. S. Sarto, "shielding effectiveness of a thick multilayered panel in a reverberating environment," *IEEE Trans. Electromagn. Compat.*, vol. 53, no. 3, pp. 579–588, Aug. 2011.

[38] A. Mehdipour, I. D. Rosca, C. W. Trueman, A. Sebak, and S. Van Hoa, "Multiwall carbon nanotube-epoxy composites with high shielding effectiveness for aeronautic applications," *IEEE Trans. Electromagn. Compat.*, vol. 54, no. 1, pp. 28–36, Feb. 2012.

[39] E. Decrossas, M. A. El Sabbagh, S. M. El-Ghazaly, and V. F. Hanna, "Engineered carbon-nanotubes-based composite material for RF applications," *IEEE Trans. Electromagn. Compat.*, vol. 54, no. 1, pp. 52–59, Feb. 2012.

[40] J. P. A. Bastos and N. Sadowski, *Electromagnetic Modeling by Finite Element Method*. New York, NY, USA: Marcel Dekker, 2003.

[41] Z. S. Sacks, D. M. Kingsland, R. Lee, and J. F. Lee, "A perfectly matched anisotropic absorber for use as an absorbing boundary condition," *IEEE Trans. Antennas Propag.*, vol. 43, no. 12, pp. 1460–1463, Dec. 1995.

[42] M. Bornert, T. Bretheau, and P. Gilormini, *Homogénéisation en Mécanique Des Matériaux*. Paris, France: Hermes Science, 2001.
[43] L. Daniel and R. Corcolle, "A note on the effective magnetic permeability of polycrystals," *IEEE Trans. Magn.*, vol. 43, no. 7, pp. 3153–3158, Jul. 2007.
[44] J. Eshelby, "The determination of the elastic field of an ellipsoidal inclusion, and related problems," in *Proc. Roy. Soc. Lond. A*, 1957, vol. 421, pp. 376–396.
[45] J. A. Stratton, *Electromagnetic Theory*. New York, NY, USA: McGraw-Hill, 1941.
[46] A. H. Sihvola and I. V. Lindell, "Electrostatic of an anisotropic ellipsoid in an anisotropic environment," *AE Int. J. Electron. Commun.*, vol. 50, no. 5, pp. 289–292, 1996.
[47] C. L. Holloway and E. F. Kuester, "Impedance-type boundary conditions for a periodic interface between a dielectric and a highly conducting medium," *IEEE Trans. Antennas Propag.*, vol. 48, no. 10, pp. 1660–1672, Oct. 2000.
[48] M. Johansson, C. L. Holloway, and E. F. Kuester, "Effective electromagnetic properties of honeycomb composites, and hollow-pyramidal and alternating-wedge absorbers," *IEEE Trans. Antennas Propag.*, vol. 53, no. 2, pp. 728–736, Feb. 2005.
[49] T. Mori and R. Tanaka, "Average stress in matrix and average elastic energy of materials with misfitting inclusions," *Acta Metall. Mater*, vol. 21, pp. 597–629, 1973.

Authors' photographs and biographies not available at the time of publication.